

# IMPROVED FATIGUE TEST SPECIMENS WITH MINIMUM STRESS CONCENTRATION EFFECTS<sup>1</sup>

Daniel de Albuquerque Simões<sup>2</sup>  
Jaime Tupiassú Pinho de Castro<sup>3</sup>  
Marco Antonio Meggiolaro<sup>3</sup>

## Abstract

The American Standard for Testing and Materials (ASTM) has standardized numerous mechanical tests such as the constant amplitude axial fatigue test of metallic materials (E 466–96), the strain-controlled fatigue testing (E 606–92) and the strain-controlled axial-torsional fatigue testing with thin-walled tubular specimens (E 2207–02). The specimens for such tests must have notches to connect their uniform test section to the larger heads required to grip them. The usual practice is to specify notches with as large as possible constant radius roots, since they can be easily fabricated in traditional machine tools. However, notches with properly specified variable radius may have much lower stress concentration factors than those obtainable by fixed notch root radii. The objective of this study is to analyze the stress distribution in these specimens using the finite element method and to quantify the stress concentration improvements achievable by optimizing variable radius notches for typical push-pull, rotary bending and alternate bending fatigue test specimens by redesigning the specimen geometry without changing their overall dimensions.

**Key words:** Stress concentration factor; Shape optimization; Finite element methods.

## CORPOS DE PROVA DE FADIGA COM CONCENTRAÇÃO DE TENSÃO REDUZIDA

### Resumo

A ASTM (*The American Standard for Testing and Materials*) padronizou inúmeros testes mecânicos, como por exemplo, o teste de fadiga de amplitude constante para materiais metálicos (E466–96), o teste de fadiga com deformação controlada (E 606–92) e o teste de fadiga de torção axial de corpos de prova tubulares (E 2207–02). Esses corpos de prova possuem entalhes que conectam à seção de teste a sua cabeça. A prática usual é especificar entalhes com os maiores raios possíveis, pois eles podem ser fabricados facilmente em máquinas tradicionais. Entretanto, entalhes com raios variáveis apropriados podem resultar em uma concentração de tensão muito menor do que aqueles de raio constante. O objetivo desse estudo é analisar a distribuição de tensão em corpos de prova típicos de tração, torção e flexão alternada, usando o método dos elementos finitos, quantificando a melhoria na concentração de tensão que pode ser obtida com a otimização do raio dos entalhes dos mesmos, sem modificar suas dimensões gerais.

**Palavras-chave:** Concentração de tensão; Otimização; Método dos elementos finitos.

<sup>1</sup> *Technical contribution to 67<sup>th</sup> ABM International Congress, July, 31<sup>th</sup> to August 3<sup>rd</sup>, 2012, Rio de Janeiro, RJ, Brazil.*

<sup>2</sup> *Mechanical Engineer, Master candidate at Pontifícia Universidade Católica do Rio de Janeiro, Brazil.*

<sup>3</sup> *Mechanical Engineer, Ph.D., Professor at Pontifícia Universidade Católica do Rio de Janeiro, Brazil.*

## 1 INTRODUCTION

Fatigue test specimens must have notches to connect their uniform test section to the larger heads required to grip them. Since such notches locally concentrate the nominal stress around their roots, they may localize the crack initiation point, spoiling the test results, or at least increasing their dispersion. But the constant radius notch tips, traditionally specified in most specimens to alleviate their stress concentration effects, do not minimize them. In fact, natural structural members, such as tree branches and bones, after many million years of evolution, have learned to use notches with variable radius, instead of the fixed radius notches typically used in engineering. This problem has been recognized for a long time, but variable radius notches optimized to minimize their deleterious influence on fatigue strength are not yet widely used in mechanical design.

The usual practice is to specify notches with as large as possible constant radius roots, since they can be easily fabricated in traditional machine tools. However, notches with properly specified variable radius can have much lower stress concentration factors (SCF) than those obtainable by fixed notch root radii. Therefore, such improved notches can be a very good design option to augment fatigue lives without significantly affecting the global dimensions and weight of structural components. Moreover, these improved notches are certainly more useful than ever, as nowadays they can be economically manufactured on widely available computer numerical control (CNC) machine tools. The focus of this study is to analyze, using the finite element method, the SCF improvements achievable by optimizing variable radius notches for typical push-pull, rotary bending, alternated bending, and tension-torsion fatigue test specimens.

## 2 NOTCH IMPROVEMENT FUNDAMENTALS

Notches are transitional geometric details such as holes, fillets, slots, grooves, keyways, shoulders, corners, threads, etc., inevitably found in most structural components. Despite being necessary for their functionality, such details severely affect local stress distributions by increasing, or concentrating, nominal stresses around their roots. This effect is quantified by the notch SCF  $K_t = \sigma/\sigma_n$ , where  $\sigma$  is the maximum stress at its root and  $\sigma_n$  is the nominal stress which would act there if the notch had no effect on the stress distribution. High  $K_t$  values can have a very deleterious effect on failure mechanisms such as fatigue crack initiation and brittle fracture. To mitigate such effects, abrupt geometrical transitions should be avoided, in particular by smoothing the notch tip roots, typically by rounding the notch root profiles.<sup>(1,2)</sup>

Fillets are required in fatigue test specimens (TS) to connect their uniform test section to their gripping heads. Fatigue TS frequently fail at the ends of their straight gage sections, where the fillet curvature starts. Such failures depend on the fillet  $K_t$ , and may lead to underestimate material fatigue strengths and to higher dispersion of the tests results. To control such problems, standard ASTM test specimens use circular arc fillets with radii much larger than their diameter or width (if rectangular).<sup>(3)</sup> The shape of trees inspired Mattheck<sup>(4)</sup> to better understand how nature improves their roots, barks and branches. He showed that this concept could be also applied in engineering design, by copying the tree self-growth mechanism to improve notch shapes in structural components.<sup>(5)</sup> Based on the trees preference for triangular shaped geometrical transitions (Figure 1), Mattheck developed a simple, but efficient

graphical way of creating variable radius fillets, called the method of tensile triangles (Figure 2).

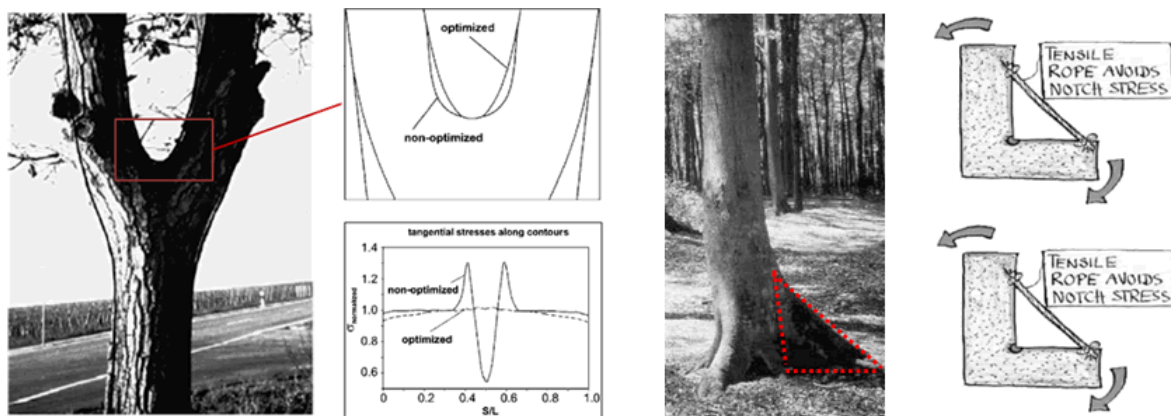


**Figure 1.** Tree geometry optimization observed by Mattheck: nature adds material where the stress is high and removes it where the stress is low. Trees like to use triangular shaped reinforcements.<sup>(4)</sup>

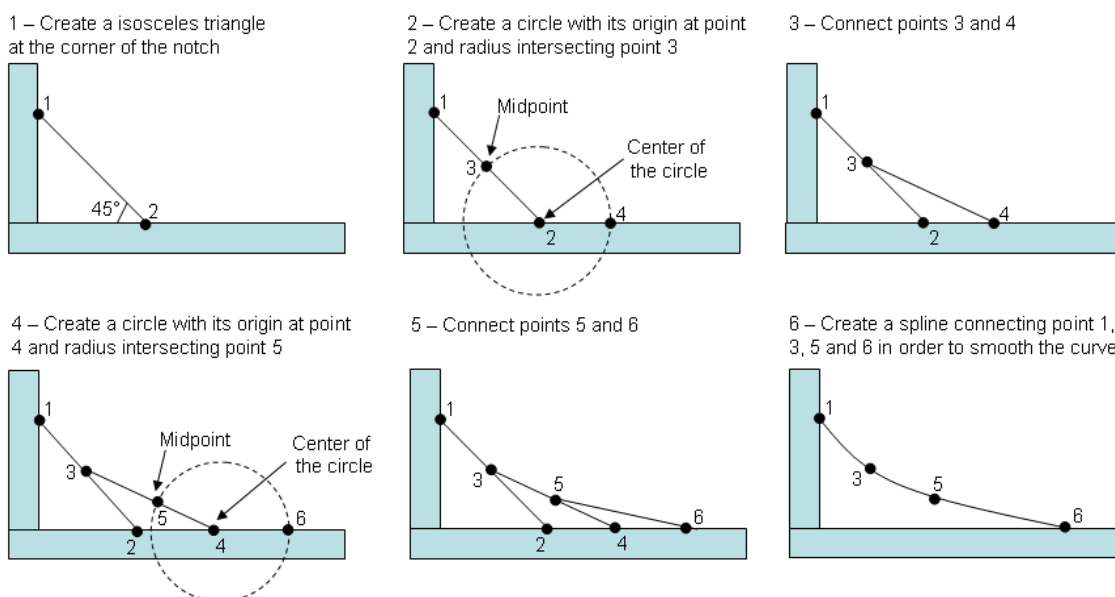


**Figure 2.** Mattheck's tensile triangle method.

Pilkey<sup>(1)</sup> mentions that Grodzinski proposed another graphical method to create variable radius fillets, by dividing the geometrical transition region in a number of equally spaced but not necessarily identical intervals connected by straight lines (Figure 3).

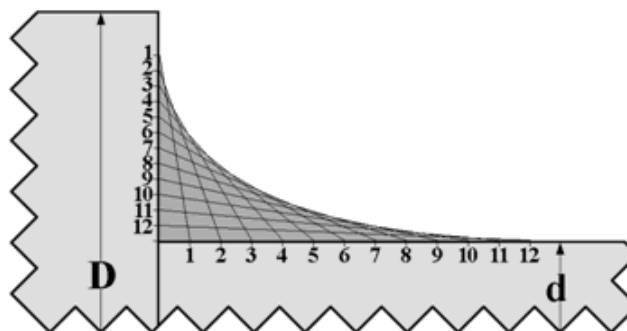


**Figure 3.** Grodzinski's variable radius curve.

Progressive curvature fillets with constant stress along the profile may be designed, possibly even reducing their SCF to unit by using transitioning fillet radii much larger than the testing section diameter.<sup>(2,6)</sup>

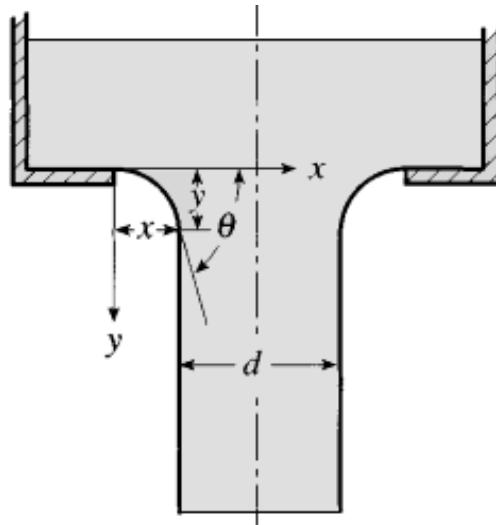


Figure 4. Liquid flowing from an opening in a bottom tank.<sup>(1)</sup>

A procedure proposed by Baud a long time ago is based on a hydrodynamic analogy. He assumed that the shoulder fillet may be compared to a free jet of water flowing under laminar steady state conditions through an opening in a bottom of a large tank (Figure 4). The constant water velocity at the jet boundary may be seen as analogous to the constant stress along a fillet boundary in a mechanical component. This hydrodynamic problem has an exact mathematical solution, and thus the x-y coordinates of the water jet boundary may be obtained from Equations 1 and 2, where  $d$  is the smallest shoulder diameter and  $\theta$  is the angle between the tangent to the fillet and the x-axis. These equations are valid only for values of  $\theta$  between zero and an angle infinitely smaller than  $\pi/2$ , because as  $\theta$  approaches  $\pi/2$  the value of  $y$  tends to infinite, therefore the curve needs to be slightly adjusted in order to enable a smooth fillet transition into the y-axis.<sup>(6)</sup>

$$x = 2 \frac{d}{\pi} \sin^2 \frac{\theta}{2} \quad (1)$$

$$y = \frac{d}{\pi} \left[ \log \tan \left( \frac{\theta}{2} + \frac{\pi}{4} \right) - \sin \theta \right] \quad (2)$$

Figure 5 shows the stress concentration effects on the stress distribution along a shoulder fillet on a flat bar pulled by a centered tensile load, calculated by a refined finite element analysis, for the improved variable radii fillets proposed by Mattheck, Grodzinski, and Baud, and for the traditional quarter-circular one.

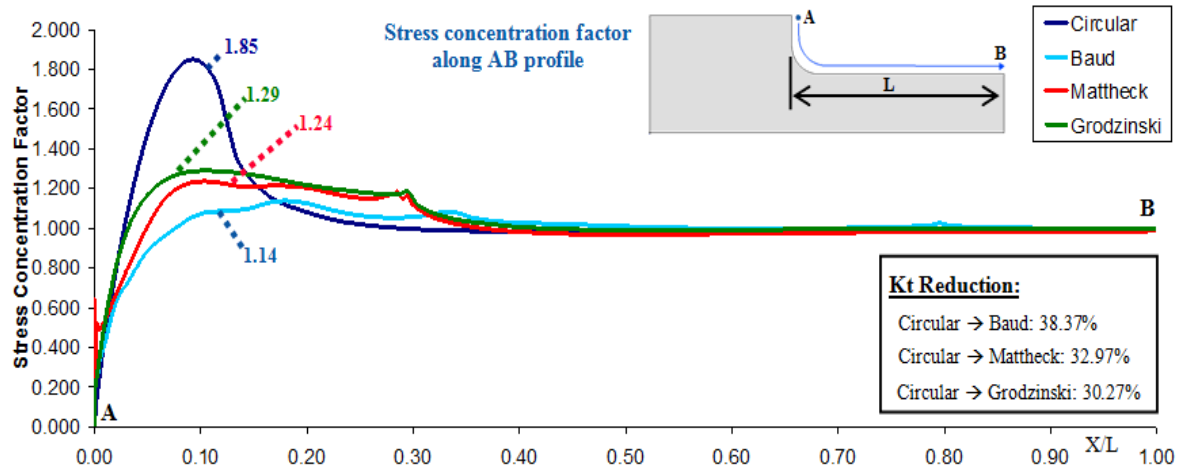


Figure 5. Comparison between improved variable radii and the traditional quarter-circular fillets.

Despite their much higher efficiency to reduce stress concentration effects around unavoidable notches, these variable radii fillets have been neglected by most modern designers. However, if correctly applied, they can considerably decrease their SCF, and consequently increase fatigue lives of structural components at a very attractive cost.

### 3 SHAPE OPTIMIZATION TO REDUCE STRESS CONCENTRATION EFFECTS

According to Baud's hypothesis that a constant tangential stress results in the minimum SCF, the notch tip curvature should not be assumed beforehand circular. It should instead be numerically optimized to reach a quasi-uniform tangential stress, reducing the peak stress to a minimum. This assumption is proved by the fade-away law proposed by Neuber, which states that the curvature of the notch profile has a large influence on the peak stress, whereas only part of the notch boundary influences the peak stress. He also showed that the higher the peak stress at the notch is, the more the stresses fade away as the distance from the notch root increases. Thus, spots at large distance from the notch have little influence on the peak stress.

Many studies on shape optimization to reduce SCF based on different approaches led to almost identical results. Sonmez<sup>(7,8)</sup> based his optimization process on a stochastic algorithm called the direct search simulated annealing, which relies on a thermodynamic analogy to search for the lowest energy state, looking for a fillet boundary shape that results in a minimum tangential stress. Das et al.<sup>(9)</sup> used evolutionary structural optimization (ESO) algorithms based on the concept of slowly removing inefficient materials from a structure to lead it towards an optimum shape. Figure 6 shows a photo-elastic model with an optimum fillet profile. This profile was optimized from an initial circular notch root, producing an almost uniform tangential stress along its boundary.<sup>(10)</sup>



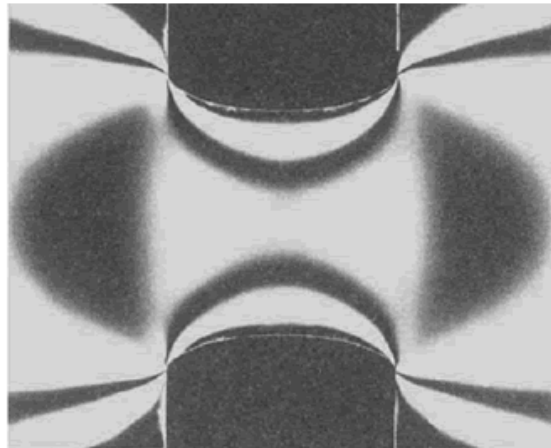


Figure 6. Isochromatic lines in a tensile bar with optimum notches.<sup>(10)</sup>

Optimization algorithms, such as the so-called gradientless algorithm, may be used to iteratively add material where the stresses are higher than desired, and to remove it where the stresses are too low.<sup>(11-13)</sup> The optimization problem is to find the shape of the transition fillet that minimizes the notch SCF. The objective function is the tangential or the Mises stress along the fillet profile, which must be as uniform as possible to meet Baud and Neuber's criteria. In gradientless methods, stress derivatives are not needed, which simplifies the optimization process. Instead, the design boundary may be simply modeled with cubic splines, defined by control points distributed along the notch profile. The optimal shape is achieved iteratively by moving the points along the fillet using an algorithm that simulates the growth of material found in natural structures.<sup>(11)</sup>

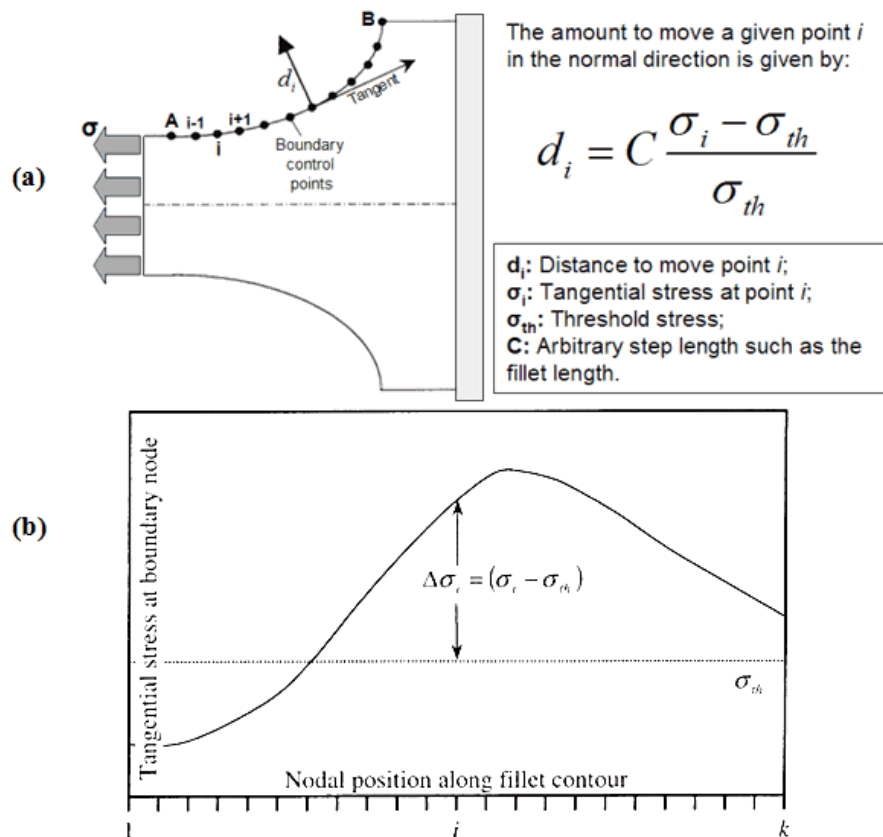


Figure 7. (a) Gradientless shape optimization method in a loaded plate; and (b) tangential stress along fillet contour modified.<sup>(12)</sup>

Figure 7a shows a flat bar with a shoulder fillet divided in control points, subjected to a remote tension loading. The tangential stress along this initial fillet varies significantly along its contour (Figure 7b). The gradientless optimization method seeks a constant tangential stress along the fillet by moving its control points by an appropriate amount ( $d_i$ ) defined by the simple equation presented in Figure 7a. The movement of any given point ( $i$ ) in its normal direction depends on its tangential stress ( $\sigma_i$ ) and on a specified threshold stress ( $\sigma_{th}$ ) at point A, which does not move during the optimization process. A factor C may be used to accelerate the optimization process. This is an iterative process, since the stress at each point of the boundary is calculated at every iteration and compared with the desired reference stress. If it is lower, material is removed from that point (negative  $d_i$ ); if it is higher, material is added to it (positive  $d_i$ ).

#### 4 FATIGUE TEST SPECIMENS

This study aims to study the stress distribution on standard fatigue test specimens, as well as to find ways of improving their geometry in order to reduce stress concentration effects at their fillet notch roots. The fatigue test specimens studied are numbered from I to V (Figure 8). Specimens I thru IV are ASTM standard fatigue test specimens and specimen V is a generic bending fatigue flat bar specimen, whose dimensions are described in Table 1.

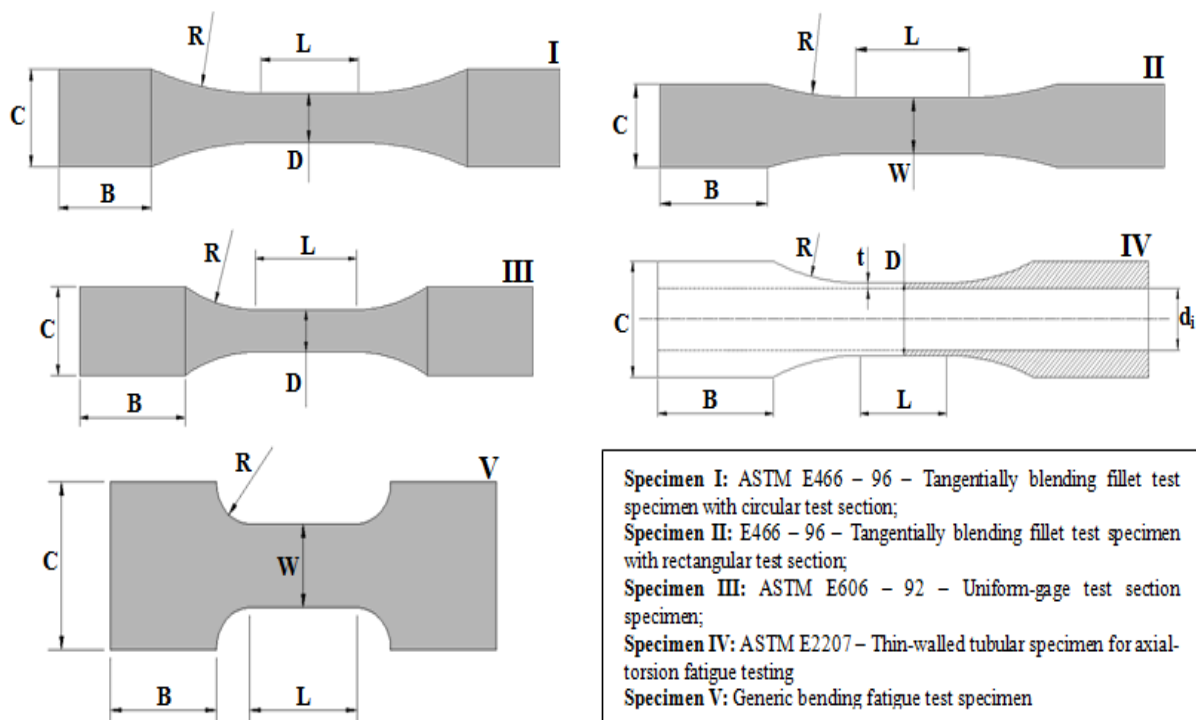


Figure 8. Fatigue test specimens studied in this work. <sup>(14-16)</sup>

**Table 1.** Fatigue test specimens dimensions

Dimension (mm)	Description	Fatigue Test Specimen				
		I	II	III	IV	V
L	Length of straight section in the middle of the specimen	76.20	63.50	19.05	42.00	10.16
R	Transition radius	203.20	203.20	50.80	89.60	3.18
D	Test section diameter	25.40	NA	6.35	28.00	NA
W	Test section width	NA	25.40	NA	NA	6.35
C	Outer diameter/width	50.80	NA	12.70	44.80	12.70
B	Length of grip end	60.00	60.00	19.05	56.0	10.00
di	Inner diameter of the tube	NA	NA	NA	23.80	NA
t	Wall thickness of the thin-walled tube	NA	NA	NA	2.00	NA

The specimens were modeled in ANSYS APDL version 12 under plane stress conditions, using triangular shaped, six-node, and twelve degree of freedom elements. Due to their symmetry, only one quarter of the specimens needed to be modeled. Figure 9 shows the finite element models for each one of the 5 test specimens studied. Models I and III have circular profiles and their geometry and load are axisymmetric about the y-axis; model II has a rectangular profile symmetric about the y-axis; model IV has a tubular profile axisymmetric about the y-axis; and model V has a rectangular profile anti-symmetric about the y-axis for its bending load conditions.

## 5 RESULTS AND DISCUSSION

Standardized fatigue test specimens use the traditional quarter-circular arc to connect their uniform test section to the larger heads required to grip them in the testing machines. Their fillets are specified with generous constant radii that decrease, but not minimize their SCF. Figure 10 shows the SCF plots resulting from each one of the finite element models for the standard TS described in the previous section. The SCF was obtained by dividing the peak stress (at the notch root) by the nominal stress. Note how the stresses vary along the notches profile.

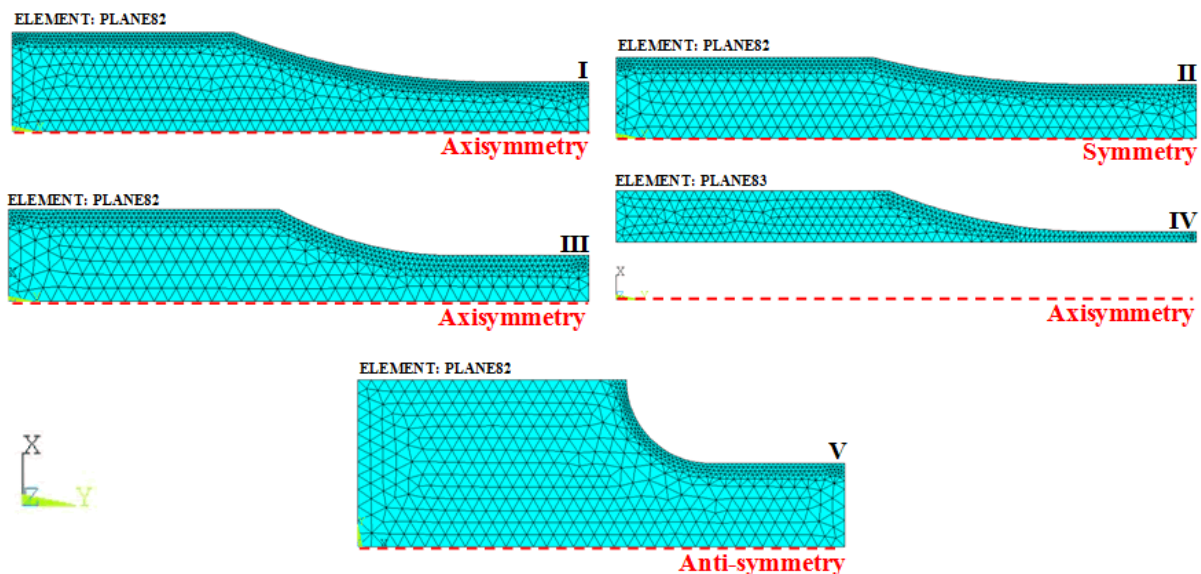


**Figure 9.** Standard fatigue test specimens finite element models.



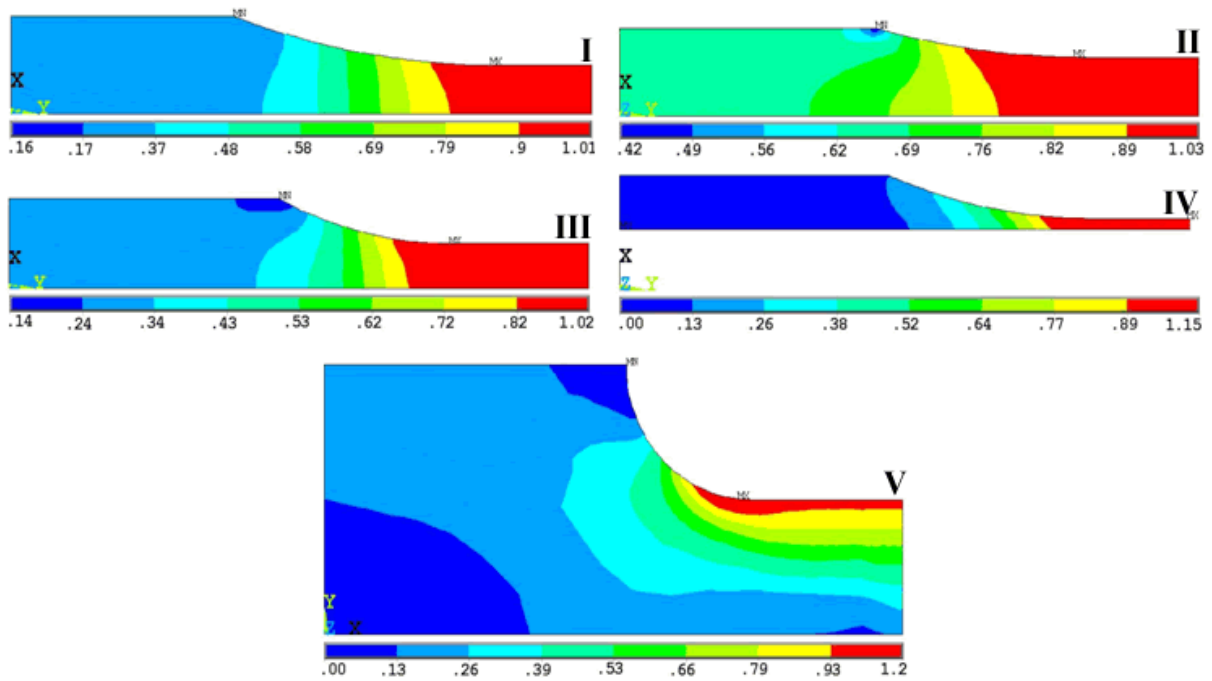


**Figure 10.** SCF along the circular radii fillets of standard fatigue specimens.

Figure 11 shows the SCF plots for the optimized fillets, all with variable radii geometries. Note how smoother the stresses are along such improved profiles.

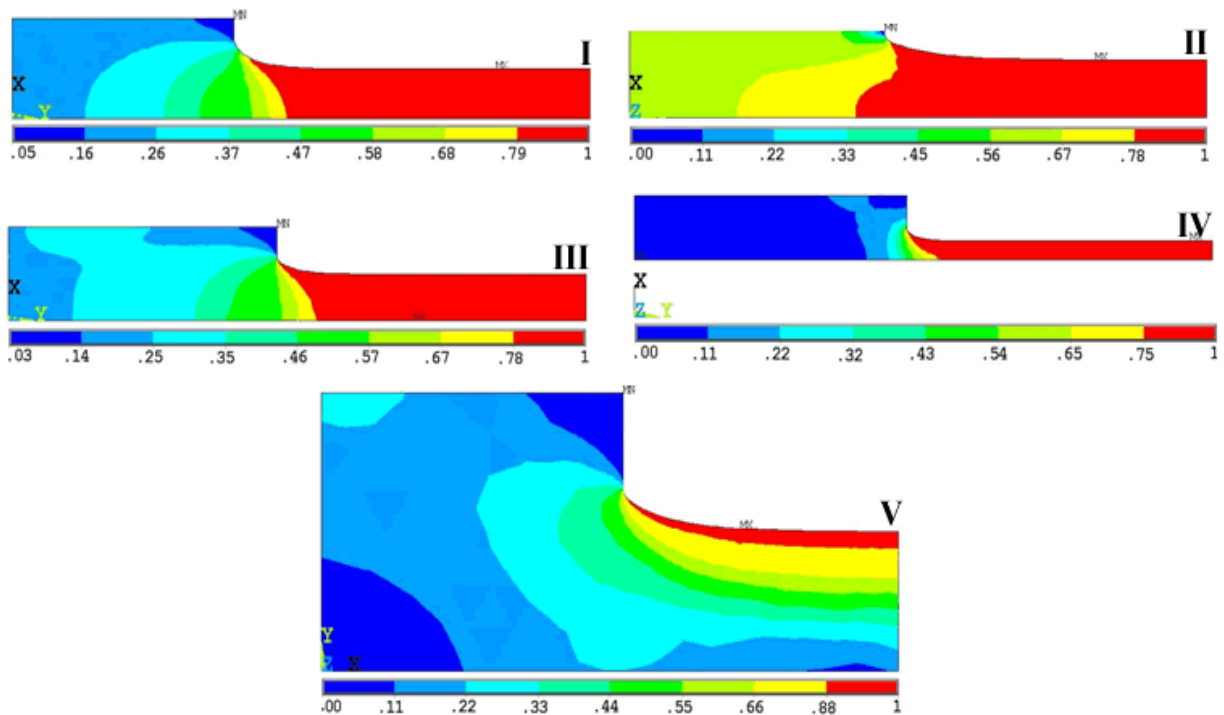


**Figure 11.** SCF along the variable radii fillets of the optimized fatigue specimens.

Figure 12 shows the SCF along the boundary fillet for each one of the TS, comparing both the original and optimized fillets. Although the SCF is almost the same, the stress distribution along the optimized boundary is practically constant along the entire fillet.

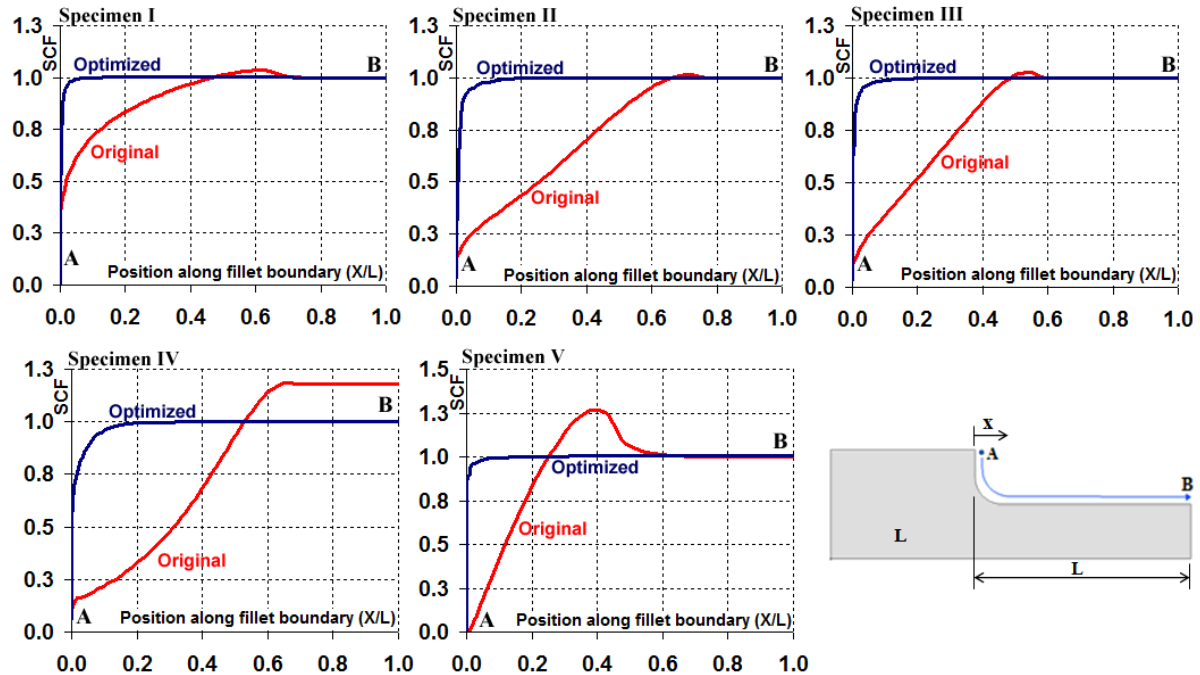


Figure 12. Mises stress along fillet boundary.

Figure 13 shows a chart that compares 7 different hypothetical transitioning fillets, each one of them with a different ratio between its radius and specimen test section width, in order to show the  $R/W$  ratio influence on the SCF for the ASTM 466 TS (specimen II), which has a low  $C/W$  ratio. As it may be seen, for the quarter-circle fillet with  $R/W = 0.25$ , the SCF reaches a value of about 1.8. As the  $R/W$  ratio increases, the  $K_t$  reduces considerably, until it almost reaches unit when  $R/W \cong 8$ , which explains why ASTM specified this as the minimum fillet radius. This clearly shows that the traditional quarter-circle fillet is far from the best choice to be used as the transitioning geometry. However, as the TS radius increases, its required overall length (RL) also increases.

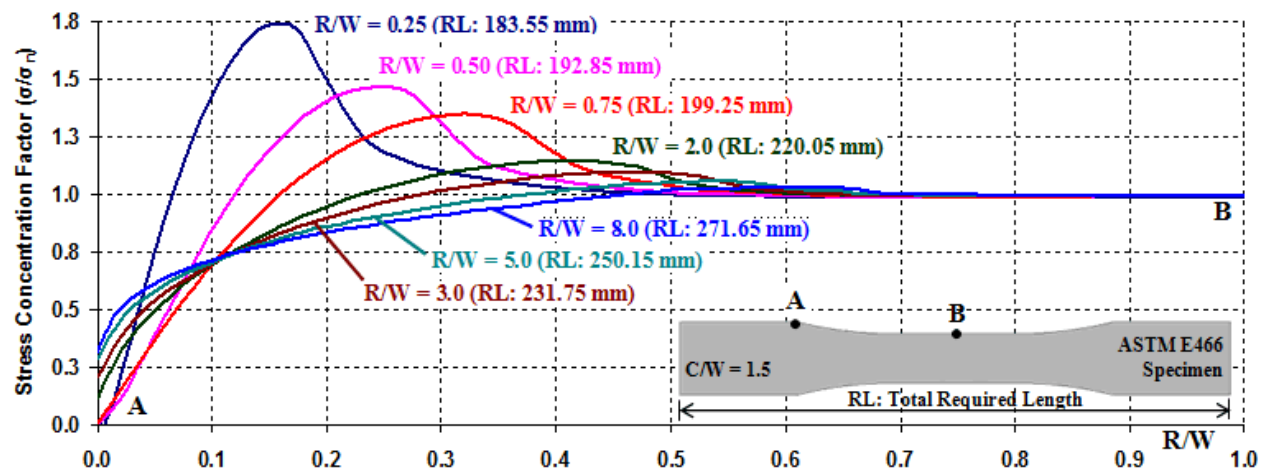


Figure 13. Stress concentration factor along the boundary fillet for original specimen.

Specimens with low  $C/W$  ratios (Figure 13), typically have large radius arc in order to reduce the SCF. ASTM standard specimens have low  $C/W$  ratio, thus they need to have a relatively long length. This is not good, not only since they require more material, but mainly because they are less buckle-resistant than a shorter TS.

Optimized specimens may have equally low  $K_t$  with much smaller lengths. In fact, the optimization algorithm is defined by geometrical constrains, such as length limitations.

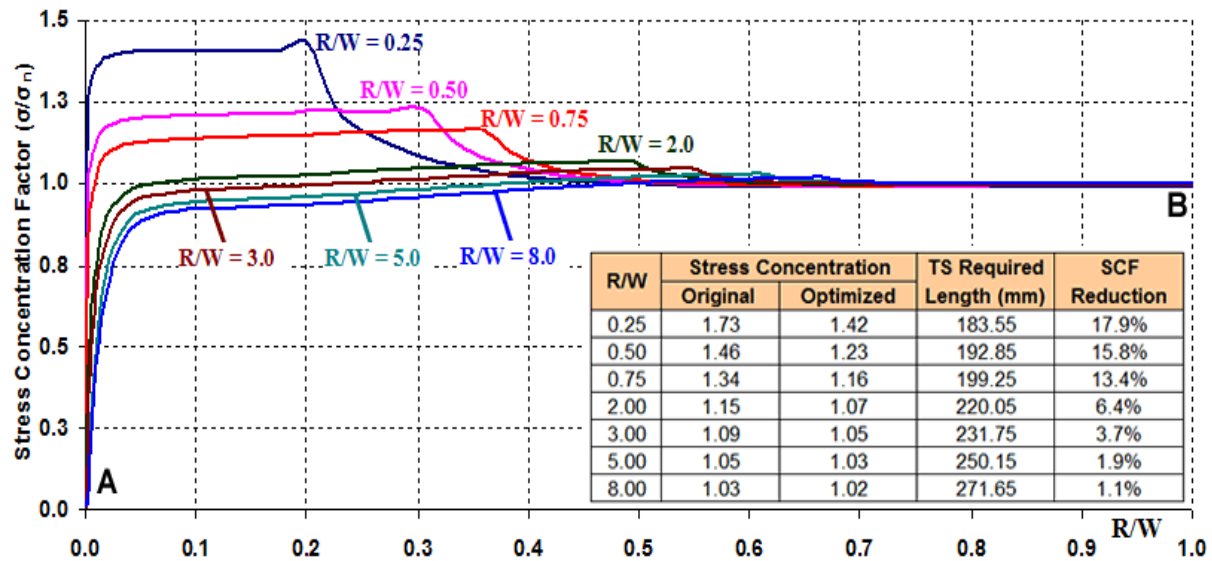


Figure 14. Stress concentration factor along the boundary fillet for original specimen.

Figure 14 shows the SCF along optimized curves for the same specimen from Figure 13, with  $R/W$  also ranging from 0.25 to 8. As it may be seen, the optimization process is quite efficient for low  $R/W$  ratio geometries; however its effectiveness reduces as the  $R/W$  ratios increases. Figure 15 supports this statement by comparing the SCF of the original and optimized ASTM 466 specimens, considering  $R/W$  ratios ranging from 0.25 thru 8 and showing the required TS length for each  $R/W$  ratio. Although the SCF reduces almost 80% from  $R/W = 0.25$  to  $R/W = 8$ , the space required for the smoother and larger fillet increases almost 1.5 times.

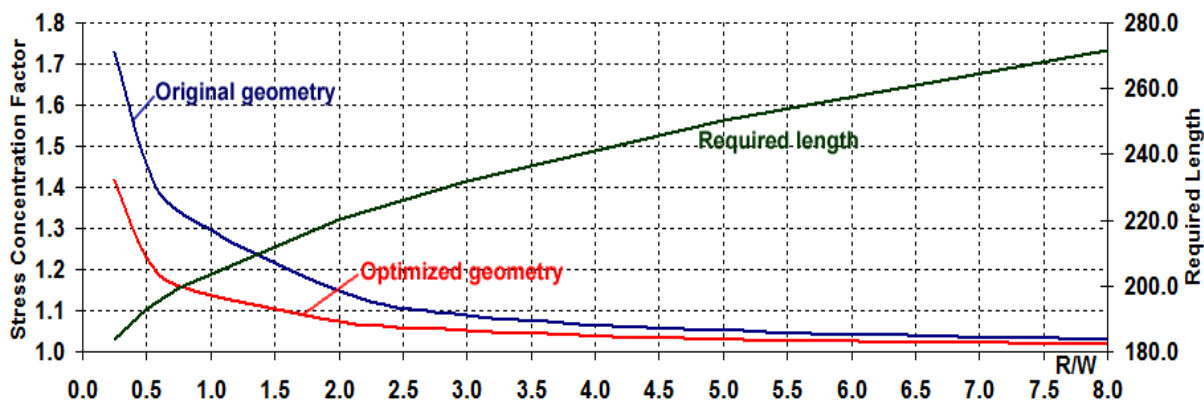


Figure 15. Stress concentration factor along the boundary fillet for optimized specimen II.

This optimization procedure results in a quite uniform tangential stress along the fillet boundary, consequently reducing the SCF to almost its minimum possible value. The optimization may be efficiently applied to components where the stress varies considerably along the fillet boundary, e.g. when the  $R/W$  ratios are low and in some cases, when it is not possible to use a large radius due to space limitations. Instead of searching for an academically optimum solution, it may be more interesting to find and improved but economical and feasible specimen. From Figure 15, it is possible

to find an improved fillet that leads to both a reduced SCF and low TS length. For example, considering  $R/W = 1.5$  and using the optimized geometry curve, the SCF is only 1.1 and the TS required length is about 212.95 mm, more than 21% shorter than the  $R/W = 8$  ratio, which not only results in a considerable material saving but also increases the buckling resistance. The other ASTM specimens (I, III, IV and V) considered in this study follow this same pattern and their results will not be shown in this paper due to space limitations.

## 6 CONCLUSIONS

Baud and Neuber identified a long time ago that a uniform tangential stress along notch boundaries lead to lower SCF. Following this idea, an optimization gradientless procedure was developed to add material where the stress is high and to remove it where the stress is low along the notches profile. This is a simple and very efficient way of improving notch shapes by minimizing their SCF, especially those with large section reductions and/or low  $R/W$  ratios. For ASTM TS with high  $R/W$  ratio, an alternative and suitable improved fillet may be obtained from this optimization process. Despite of not being the optimum solution, it is much better than the one obtained from the tradition quarter-circle fillet and moreover it uses much less material than the default  $R/W = 8$  ration widely used by ASTM standard TS. Considering, for instance, a workshop that needs to test several TS, this length reduction may lead to large economical savings without compromising the overall fatigue test results.

## Acknowledgements

CNPq provided research scholarships, ABS Group Services do Brasil, especially his supervisor Viviane Krzonkalla, supported this work allowing research time for his employee, who received a tuition-free scholarship from PUC-Rio.

## REFERENCES

- 1 Pilkey, W.D., 1997. Peterson's stress concentration factors, 2nd ed., Wiley.
- 2 Lansard, R. Fillets without stress concentration, Laboratoires de la Société des Automobiles Peugeot, 1954
- 3 Garrell, M., Shih, A., Curzio, E.L., Scattergood, R., Finite element analysis of stress concentration in ASTM D 638 tension specimens, J of Testing Materials, 2003, Vol. 31, No 1
- 4 Mattheck, C., 2006. Teacher tree: The evolution of notch shape optimization from complex to simple, Engineering Fracture Mechanics, vol. 73, No12, pp. 1732-1242.
- 5 Mattheck, C.; Burkhardt, S., 1990. A new method of structural shape optimization based on biological growth, Int J of Fatigue, vol. 12, No 3, pp. 185-190.
- 6 Baud, R.V., Fillets profiles for constant stress, Product engineering, 1934; April, p. 133-134
- 7 Sonmez, F., Structural optimization using simulated annealing, 2008, Simulated annealing, pp. 420, I-Tech education and publishing
- 8 Sonmez, F., Shape optimization of 2D structures using simulated annealing, 2007, Computer methods in applied mechanics and engineering, pp. 3279-3299
- 9 Das, R., Jones, R., Xie, Y.M., Design of structures for optimal static strength using ESO, 2005, Engineering failure analysis, pp. 61-80

- 10 Schnack, E., An optimization procedure for stress concentration by the finite element technique, Int J for numerical methods in engineering, 1979, vol. 14, pp. 115-124
- 11 Heller, M., Kaye, R. and Rose, L.R.F., 1999. A gradientless finite element procedure for shape optimization, J of strain analysis, vol. 34, No 5, pp. 323-336.
- 12 Waldman, W., Heller, M., and Chen, G.X. 2000. Optimal free-form shapes for shoulder fillet in flat plates under tension and bending, Int J of Fatigue, vol. 23, No 6, pp. 509-523
- 13 Wu, Zhixue, On the optimization problem of fillets and holes in plates with curvatures constraints, 2008, Struct Multidisc Optim, 35:499-506
- 14 ASTM E 606 – 92: Standard practice for strain-controlled fatigue testing, Annual Book of ASTM Standards, West Conshohocken, PA, 1993
- 15 ASTM E 2207 – 02: Standard practice for strain-controlled axial-torsional fatigue testing with thin-walled tubular specimens, Annual Book of ASTM Standards, West Conshohocken, PA, 2002
- 16 ASTM E 606 – 92: Standard practice for controlled constant amplitude axial fatigue test of metallic materials, Annual Book of ASTM Standards, West Conshohocken, PA, 2002